

Transient-photocurrent studies in *a*-Si:H

P. B. Kirby and W. Paul

Division of Applied Sciences, Harvard University, Cambridge, Massachusetts 02138

(Received 9 May 1983)

We present a detailed study of carrier transport in sputtered *a*-Si:H with the use of the time-of-flight technique. Charge-collection experiments reveal that total charge collection must take place to enable the extraction of reliable dispersion parameters. Under this condition the dispersion parameters accurately follow the predictions of a multiple trapping and release transport process. By integration of the current transients we derive values of the $\mu_D\tau_D$ product for samples having a range of deep-state densities and also obtain the capture cross section of the dominant defect. Upon phosphorus doping the electron carrier lifetime increases; furthermore, changes in the dispersion parameters suggest that the conduction-band-tail-state distribution is altered with respect to the undoped material. We also present measurements of photocurrents made with the use of electrode coplanar geometry and suggest that carrier loss to deep states dominates the response at room temperature.

I. INTRODUCTION

The time-of-flight (TOF) technique is an excellent method for studying carrier motion in highly resistive semiconductors.^{1,2} Early investigations using TOF concentrated on observing the motion of carriers in response to externally applied fields to obtain their drift mobilities.¹ In the standard TOF experiment carriers are photoinjected near one electrode of a sample in sandwich configuration and drift under the applied electric field to the opposite electrode. A displacement current is observed in the external circuit up to the time that the carriers reach the collecting electrode. This transit time τ_T can then be used to obtain the drift mobility μ_D using

$$\tau_T = d / \mu_D E, \quad (1)$$

where d is the sample thickness and E is the applied electric field.

The photocurrent measured in a TOF experiment is given by

$$I(t) = n(t) e \mu_0 E, \quad (2)$$

where $n(t)$ is the number of mobile carriers at any time and μ_0 is the mobility of carriers in conducting states. It has been found to be common in amorphous semiconductors for the photocurrent to decrease continuously following optical excitation, a decrease that has nothing to do with carrier collection at the electrodes. Such monotonically decreasing currents were furthermore often found to be algebraic in time,²

$$I(t) \propto \begin{cases} t^{-(1-\alpha_{\text{init}})}, & t < \tau_T \\ t^{-(1+\alpha_{\text{final}})}, & t > \tau_T. \end{cases} \quad (3)$$

It is conventional to replace $n(t)\mu_0$ by $n(0)\mu_D(t)$ and refer to the mobility as time dependent and the carrier motion as dispersive. Considerable insight was achieved by Scher and Montroll³ who pointed out that such current relation-

ships could be understood with a waiting-time distribution function of the form

$$\psi(t) \propto 1/t^{1+\alpha}. \quad (4)$$

Detailed understanding of the time dependence of the photocurrent then comes through obtaining $\psi(t)$ for the sample under study. If carrier transport takes place after release from trapping states (followed by trapping a short time later) into conducting states, $\psi(t)$ will contain information on the distribution of trapping states. In fact the algebraic time dependences of the photocurrent observed in device-grade glow-discharge *a*-Si:H have been successfully interpreted in terms of carrier trapping and release in an exponential distribution (in energy) of localized states,⁴ when conduction takes place above the mobility edge in extended states.

The properties of *a*-Si:H are a sensitive function of the preparation conditions. Indeed our previous study of TOF on *a*-Si:H films prepared by the sputtering process revealed photocurrents $I(t)$ that depended on the preparation conditions and also on the applied electric field.⁵ In that study it was not possible to show conclusively whether the behavior was due to real variations in sample properties, particularly the density of deep states, or a true field-dependent dispersion.^{5,6} In the TOF context a deep state is understood to be one at which carriers, once captured, are not released within the time scale of the measurement. In Sec. III A we combine the recorded $I(t)$ measurements with measurements of collected charge $\int I dt$ to show that field-dependent $I(t)$ can be explained by carrier loss to deep states. Investigation of different samples with varying defect-state densities, as well as TOF with different electrode configurations, allow us to stipulate the condition that complete charge collection must be fulfilled for the extraction of reliable dispersion parameters from the recorded $I(t)$.

In Sec. III B we use this criterion to obtain reliable dispersion parameters versus temperature in sputtered *a*-Si:H. A linear variation of α_{init} is observed between 130

and 260 K, which, as predicted by multiple trapping and release transport models, extrapolates through zero. Both $I(t)$ and drift-mobility measurements suggest a change in the transport process below 130 K.

Charge-collection experiments have recently been performed on glow-discharge-prepared *a*-Si:H and interpreted with a Hecht analysis of carrier loss⁷ during transit to obtain the capture cross section of deep defects in this material.⁸ In Sec. III C we apply this analysis to charge-collection experiments on sputtered *a*-Si:H films and obtain trapping parameters that are similar to those found in glow-discharge material. We find that the capture cross section of the deep states is independent of temperature.

Recent experiments⁹ have shown that dispersive transport can be studied by observing the time dependence of the photocurrent following pulsed excitation with coplanar electrodes applied to the surface of the sample. In this case, as opposed to TOF, the excited carriers are created uniformly between the electrodes so that oppositely charged carriers coexist in the same region of space. In fact in *a*-As₂Se₃ it has proved possible to obtain values of $\mu_D(t)$, α , and μ_0 from coplanar measurements which are identical to those obtained in TOF.¹⁰ To date this has not been achieved for *a*-Si:H. Additionally the overlapping of the electron and hole distributions made a full study of recombination possible. In Sec. III E we present measurements of transient photoconductivity on *a*-Si:H in the coplanar geometry and suggest that the high-temperature current decays in undoped material are affected by the loss of carriers to deep states. Such considerations do not apply to phosphorus-doped material since the electron lifetime is increased by phosphorus doping, a fact which is confirmed by both TOF and coplanar photocurrent measurements.

II. EXPERIMENTAL

The samples used were prepared by sputtering in a hydrogen-argon atmosphere and characterized using techniques already published.¹¹ The photocurrents in TOF experiments were excited with an 8-ns light pulse of wavelength 5200 Å from a nitrogen-pumped dye laser. For our samples the light at this wavelength is absorbed within 2000 Å. Light levels were approximately 2 orders of magnitude below those where the light intensity influences the form of the decays, and the incident-light intensity was estimated to be approximately 10^8 photons/cm². All TOF transients reported here are independent of space-charge effects due to previous light exposure. The photocurrents after amplification were recorded with a Tektronix 7612D digitizer interfaced to a Digital Equipment Corporation computer. Generally low repetition rates (~ 1 Hz) were used and the photocurrent signals were averaged many times both to improve the signal-to-noise ratio, and to average out pulse-to-pulse laser variations. When displacement currents due to the reverse voltage pulses were unavoidably present, this background was subtracted from the displacement signal due to carrier drift.

Coplanar electrode measurements of photocurrent decays were detected on the same system. Ohmicity of the evaporated chromium contacts was assumed from in-

dependence of the photocurrent decays to the applied field. Samples were annealed at 180°C for a few hours before their study.

III. RESULTS AND DISCUSSION

A. Photocurrents in *a*-Si:H

In this section we show how photocurrents in the TOF experiment can be affected by carrier loss through bulk and surface trapping as well as barrier and surface fields. By our measurements of charge collection as a function of applied field and observations of the time dependence of the photocurrent using different contact structures we are able to separate out many of the influences on the photocurrent transients and to arrive at a reliable determination of the parameters in Eq. (3).

Figures 1(a)–1(c) show photocurrent transients recorded in three samples at different applied fields. The measurement temperature of 250 K was chosen for adequate time resolution of the phototransients in order to minimize the consequences of any rise-time distortions at $t < 50$ ns. For sample 195 under high electric fields we observe two linear regimes separated by an abrupt knee when the phototransients are plotted in units of $\log I$ vs $\log t$. The knee corresponds to drifting carriers reaching the back contact since τ_{knee} is found to decrease approximately inversely with the applied voltage.¹² It is clear from Fig. 1(a) that above 4×10^4 V/cm both the pre-transit and post-transit slopes are independent of the magnitude of the applied electric field. At high electric fields then it is worthwhile to define a unique parameter α from the initial and final slopes by the relations given in Eq. (3). At lower applied fields the phototransient shape becomes field dependent and it is not possible to define unique dispersion parameters. It is possible to identify the cause of the low-field variations from measurements of the quantity of displaced charge, which can be obtained by integration ($\int I dt$) of the measured phototransients. The results are displayed in Fig. 2. It is then clear that the observed field-dependent phototransients (e.g., $E < 4 \times 10^4$ V/cm for sample 195) can be associated with a voltage-dependent collection efficiency. The most straightforward interpretation of the results is that carrier loss is occurring during transit at sites whose thermal release times are long compared to the transit time. It is clear from these results that confidence cannot be placed in dispersion parameters derived from TOF measurements unless the possibility and consequences of carrier loss from the transport states being probed has been investigated.

In a previous study⁵ we showed that for films which had large densities of defect states ($N_{EF} > 10^{17}$ cm⁻³ eV⁻¹) it was not possible to obtain electron mobility values at 300 K because the transit time is obscured by carrier loss. Similar behavior is displayed in Fig. 1(c) for film 213. No feature corresponding to the successful transit of carriers across the sample is observed at any accessible fields. The link with carrier loss is again displayed in Fig. 2 where the displaced charge versus applied field shows that all of the injected charge is not collected until very high fields.

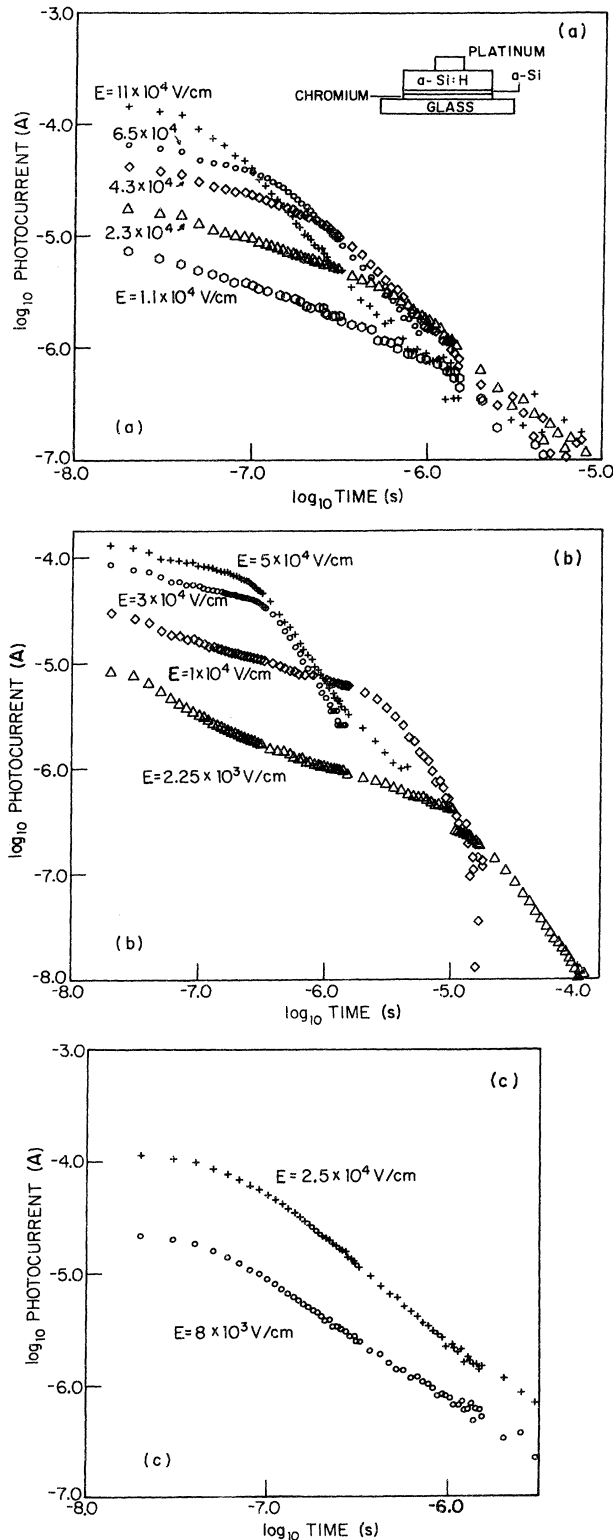


FIG. 1. (a) Transient photocurrents for electrons in sample 195 at 250 K. Sample thickness is $4.6 \mu\text{m}$. (b) Transient photocurrents for electrons in sample 217 recorded at 250 K. Sample thickness is $8 \mu\text{m}$. (c) Transient photocurrents for electrons in sample 213 recorded at 250 K. Sample thickness is $8.2 \mu\text{m}$. These transients are not the ones used to obtain the collected charge in Fig. 2.

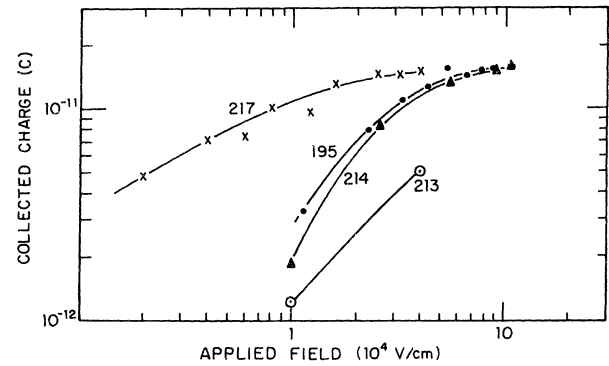


FIG. 2. Charge collection vs applied electric field for samples 217, 195, 213, and 214.

Sample 195 [Fig. 1(a)] reveals accurate algebraic decays⁹ only when the field is high enough to ensure complete charge collection. However, we will show that in other samples influences besides bulk carrier loss can lead to nonalgebraic current decays. The possible influences on the photocurrent transients include internal fields and geminate and surface recombination. We can discount geminate recombination as having significant influence in *a*-Si:H above 200 K since Fig. 2 reveals a saturated region of charge collection at high fields, whereas the theory of geminate recombination predicts the quantum efficiency for free-carrier production to be field dependent.² The quantity of charge drifting in *internal* fields can be obtained from the integral of $I(t)$ under zero applied (external) fields. For sample 195 we measure this charge to be $0.02Q_0$, where Q_0 is the maximum charge transported in the sample under high applied electric fields ($V_{\text{app}} > 6 \times 10^4 \text{ V/cm}$). Thus we do not observe the influence of the built-in field near the top platinum contact even at very short times when the carriers are moving through the region of maximum internal field.

We have seen that nonalgebraic decays can be most straightforwardly interpreted in terms of deep trapping. But on the other hand, an apparent algebraic decay does not, in and of itself, assure that no carrier loss is taking place. An example of this is shown in Fig. 1(b) where the phototransients on sample 217 are shown; this is a sample of sputtered *a*-Si:H which has the lowest density of defect states that we have measured in this laboratory. At low fields beyond (in time) the initial fast decrease the current decay is approximately algebraic up to the transit time of carriers. Below fields of $1 \times 10^4 \text{ V/cm}$ there is incomplete charge collection which then results in only small changes of the phototransients. In fact a well-defined knee corresponding to the transit time is observed down to the lowest applied fields ($2.25 \times 10^3 \text{ V/cm}$). Our previous studies on this sample⁵ with different metals as the top contact suggested (albeit indirectly) that the internal barrier field was not responsible for the initial fast decrease of the current observed at short time for fields less than $5 \times 10^3 \text{ V/cm}$. It is possible for the barrier region to influence $I(t)$ through the decrease in current that results from

carriers drifting to regions of lower internal field or by uncovering deeper states (relative to the conduction band) which act as additional capture centers for electrons. In order to ascertain the contribution of the in-built field we have produced TOF structures with an insulating blocking contact between the *a*-Si:H film and the top metal contact. A few microns of polyimide were used as the top blocking contact which after having been spun onto the surface of the *a*-Si:H had a 2-mm chromium dot evaporated onto it. $I(t)$ measurements on 217 in this configuration with zero applied field reveal very small induced currents and so there are no electric fields extending into the sample and only small surface fields ($< 10^2$ V/cm). The current transients with the organic insulator are displayed in Fig. 3. Despite the absence of an internal field the initial fast decrease of the current is still observed. The explanation of the current at short times would then seem to involve surface trapping or recombination both of which will lead to a decreasing current.

The success of the insulating layer in separating out various influences on $I(t)$ is best revealed when it is used as a blocking contact on a sample of device-quality *a*-Si:H prepared by the glow-discharge technique. When a platinum contact is applied directly to the film, $I(t)$ is strongly influenced by carrier motion in the barrier for applied fields less than 10^4 V/cm. The results for the two configurations are shown in Figs. 4(a) and 4(b). The zero-applied-field results for the Pt structure clearly reveal the presence of internal fields. The current values obtained under zero applied bias for the polyimide structure are $1\frac{1}{2}$ orders of magnitude lower than when the Pt structure is measured. The negligible current displacements due to surface fields then allow observation of current transients

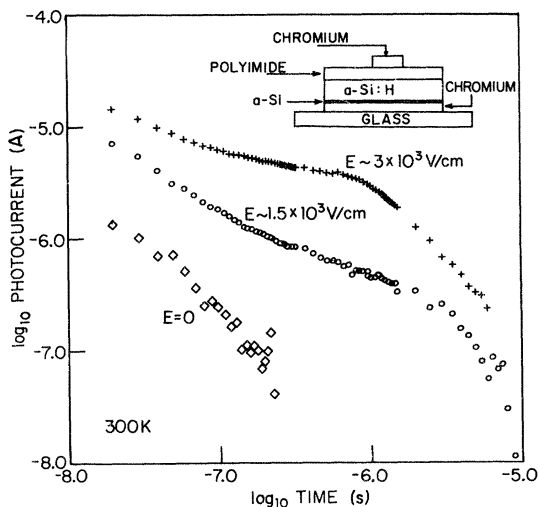


FIG. 3. Transient photocurrents for electrons in sample 217 at low fields using an organic insulator as the blocking contact. Sample structure is shown in the inset. Notice the initial fast ($< 10^{-7}$ s) decreases in the absence of a depletion field. Unfortunately the thickness of the polyimide was not known accurately, so the fields were estimated from comparison of the transit time obtained with those found in Schottky-diode structures at 300 K. Therefore their accuracy is limited.

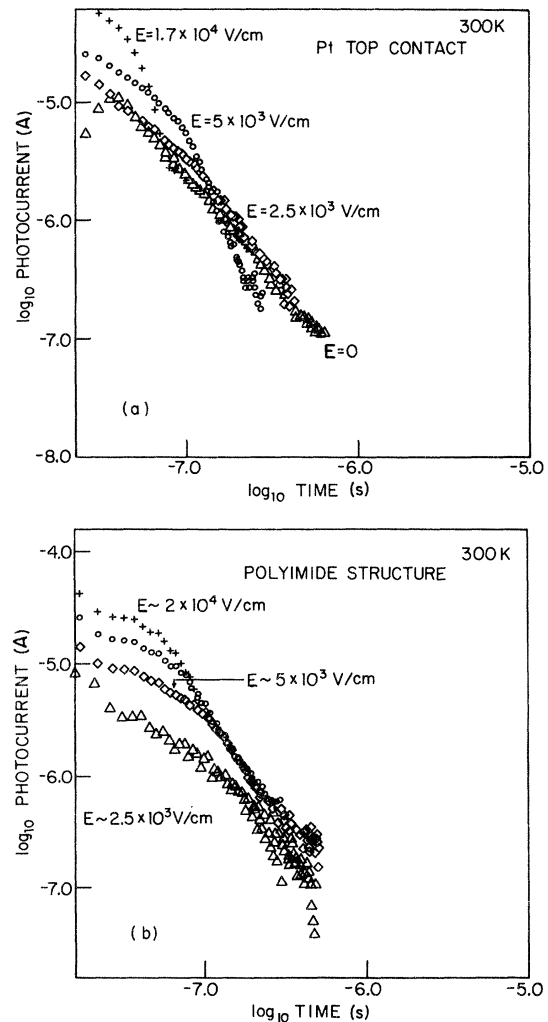


FIG. 4. (a) Transient photocurrents recorded in device-grade *a*-Si:H prepared by the glow-discharge process. Sample thickness is $4\ \mu\text{m}$. Platinum is used as the top contact. (b) Same as (a) but using polyimide as the blocking contact. Zero-field response is negligible compared to the drift signals. Again the fields are only roughly known.

at lower applied fields in the polyimide structure than when the Schottky-barrier configuration is used. The current transients at such low fields are seen to be clearly influenced by carrier loss, a conclusion that could not have definitively been reached without the structures used in this study.

We have found the polyimide structure of greater use for studying low-field phototransients than a metal-insulator-semiconductor (MIS) device formed with a thick SiO_2 layer, since our studies have shown that the oxide |*a*-Si:H interface gives rise to many surface states that trap charge, leading to severe distortion of the recorded $I(t)$ at short times. The polyimide structure used here will be particularly useful for studying the broadening of the drifting carrier packet when $\alpha_{\text{init}} = 1$ that occurs above room temperature, since such low fields can then be applied as to lengthen the transit time into experimentally

accessible time ranges. For success in this direction the investigated sample must, under the particular conditions of the experiment, show complete charge collection at such low applied fields.

We note that the observation of similar $I(t)$ independent of the presence of internal electric fields definitively proves that the observed $I(t)$ signals under study are displacement currents caused by carrier drift rather than caused by possible relaxation of internal fields.¹³

The importance of an understanding of deep trapping with regard to extraction of the dispersion parameter is also revealed in Fig. 5 for sample 213, which has significant carrier loss at the temperature of measurement ($T=200$ K). Apparently, the distribution of trapping times is so wide in this sample that, although the current decays are voltage dependent, an approximately algebraic dependence of the photocurrent on time is observed. In Fig. 1(c) showing phototransients at 250 K for sample 213, visual inspection clearly shows dominant carrier loss; however, for low-temperature transients in Fig. 5 carrier loss is only identifiable after charge-collection experiments are performed.

B. Temperature dependence of the dispersion parameters in sputtered a -Si:H

Photocurrent transients obtained using the TOF technique are usually the preferred means for obtaining the time dependence of the drift mobility in amorphous semiconductors. In this section we show the temperature dependence of the dispersion parameters (α_{init} and α_{final}) measured under the conditions of complete charge collection.

Temperature-dependent dispersion parameters are usually taken as evidence for a multiple trapping (MT) and release transport process.² For an exponential distribution of localized states descending from the mobility edge, α_{init}

is predicted to be a linear function of temperature and to extrapolate through zero.¹⁴ Furthermore, when the density of localized states is of the form

$$N_t(E) = N_0 \exp\left[-\frac{E}{kT_c}\right], \quad (5)$$

then T_c , which describes the steepness (in energy) of the trap distribution, can be obtained from TOF data since it equals the temperature at which $\alpha_{\text{init}}=1$. In this model it is assumed that the exponential distribution joins smoothly onto band states at the mobility edge so that $N_0 \sim 10^{20} \text{ cm}^{-3} \text{ eV}^{-1}$.

Typical photocurrent transients that we have observed as a function of temperature in sample 217A under conditions of complete charge collection are shown in Fig. 6. Accurate algebraic current decays are seen at all temperatures above 130 K. The dispersion parameters obtained from such data are shown in Fig. 7, and are different from previous estimates presumably due to the criteria applied in this study. The scatter in the data points is a measure of the experimental accuracy. Most scatter comes in the determination of α_{final} , whose deduction is difficult at high temperatures because of the rapid current variation with time, and is also difficult at low temperatures because of the low current values. Previous results of TOF experiments^{5,6} on sputtered a -Si:H have shown α_{init} extrapolating to zero at a finite value of temperature ~ 120 K. Although our results here do not rule out a faster variation of α_{init} to zero below 120 K, a linear variation of α_{init} between 130 and 260 K which extrapolates through zero temperature is observed as predicted by the MT theory. Extrapolating the slope of α_{init} to higher temperatures we find $\alpha_{\text{init}}=1$ at $T \sim 336$ K for the sputtered film 217A. Representative values of α_{init} that we have obtained from glow-discharge material are also shown in Fig. 7, and in agreement with previous results¹¹ give $\alpha_{\text{init}}=1$ at $T \sim 310$ K. Adopting the model of MT within an exponential state density it appears that the conduction-band-tail width of sputtered sample 217 ($T_c \sim 336$ K) is not very much different from that of glow-discharge preparations ($T_c \sim 310$ K). The MT model also predicts that the transit

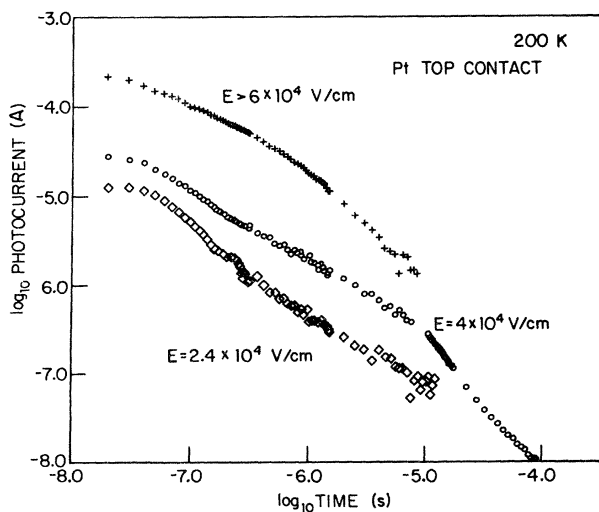


FIG. 5. Transient photocurrents in sample 213 showing the influence of carrier loss to deep traps. The measurement temperature was 200 K.

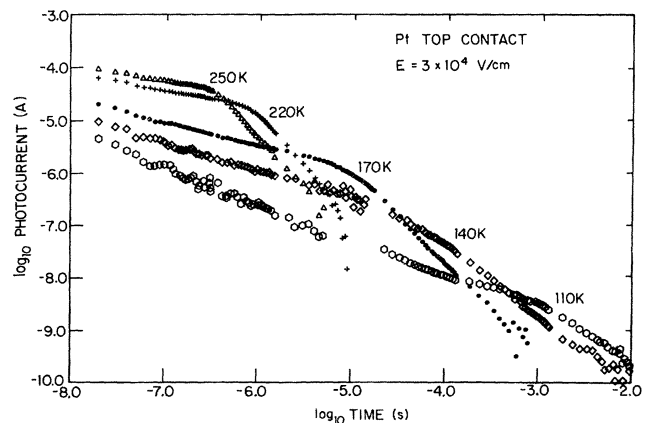


FIG. 6. Transient photocurrents in sample 217 vs temperature in the regime of complete charge collection.

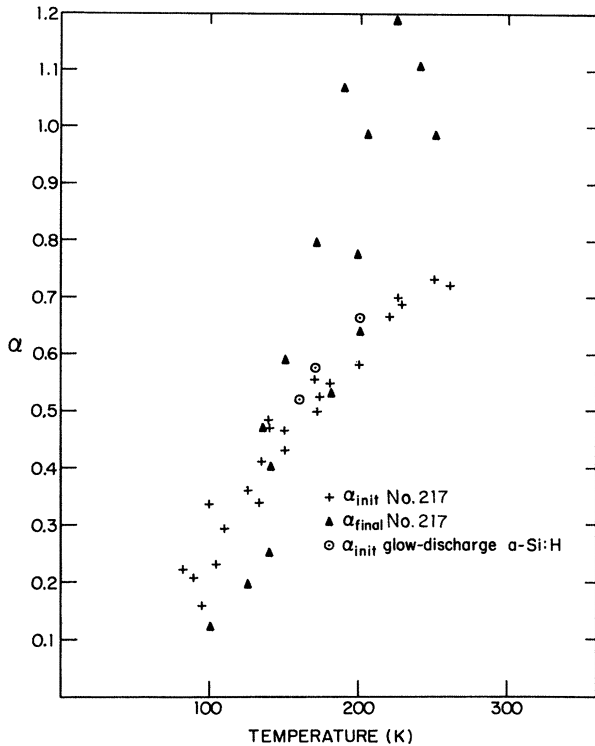


FIG. 7. Derived dispersion parameters vs temperature for sample 217A, + corresponds to α_{init} , \blacktriangle to α_{final} . Also displayed are α_{init} values for a glow-discharge-prepared sample, \circ . Values for α_{init} and α_{final} were determined manually, and at $T \equiv 130$ K, α_{init} values were obtained for $t \leq 10^{-5}$ s.

time should be field dependent for $T < 300$ K such that

$$t_T \propto E^{-1/\alpha}. \quad (6)$$

We have found that our results are accurately described by this relation at 200 K using the measured value of α_{init} at this temperature.

Electron-mobility-versus-temperature data that we have obtained on sample 217B are displayed in Fig. 8. The voltage dependence of the drift mobility is clearly seen. At the lowest temperatures ($T < 130$ K) there seems to be evidence for a change in the transport mechanism revealed by lessening of the temperature dependence of the mobility. Additional evidence for such a change is observed in the low-temperature (110 K, Fig. 6) photocurrents. After a fast fall off for times less than 10^{-5} s, the photocurrent decay is followed by a slower decay up to the transit time. This region is worthy of further study.

Between 175 and 270 K the data in Fig. 8 are fairly well described by the model of Tiedje and Rose,⁴ which predicts that the mobility should vary as

$$\mu_D \approx \mu_0(1-\alpha) \left[\frac{vt_0}{1-\alpha} \right]^{1-1/\alpha}, \quad (7)$$

for $T < 0.8T_c$ where t_0 is $d/\mu_0 E$. If we assume $\mu_0 = 13$ cm^2/Vs and $v = 4 \times 10^{12}$ s^{-1} , the values determined for

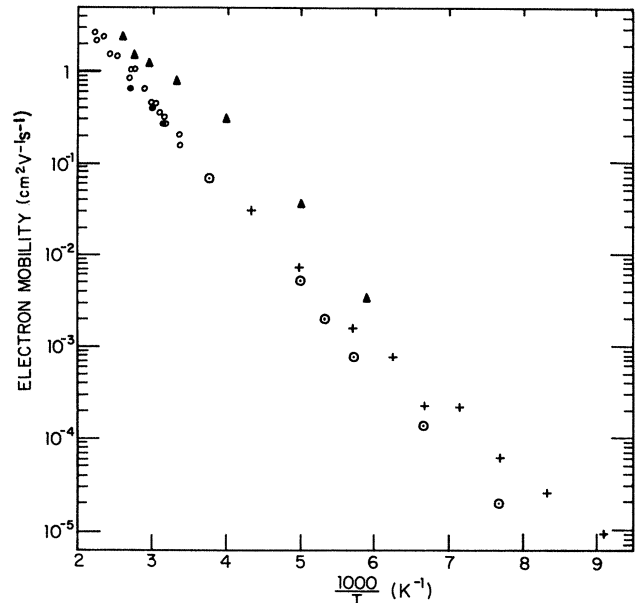


FIG. 8. Electron-drift-mobility values obtained in sample 217B (\circ , +, \bullet , and \diamond) and a glow-discharge sample (\blacktriangle), \circ , +, and \bullet correspond to 4 , 6.25×10^4 , and 3×10^4 V/cm, respectively; these applied fields are such that complete charge collection is obtained. \circ corresponds to 2.25×10^3 V/cm and incomplete charge collection. Transit times used to obtain the electron-mobility values were obtained from the intersection point of two linear regimes on a $\log I$ -vs- $\log t$ plot when the transport was dispersive and also at high temperatures for incomplete charge collection. In the temperature range where the transport is nondispersive the time at which the current drops by 50% was used as the transit time under complete-charge-collection conditions.

glow-discharge-produced material,¹⁴ a reasonable fit to the data is obtained. It thus appears that identical parameters are applicable for both glow-discharge and sputtered material, at least for the limited comparison performed so far. The phototransients recorded above 300 K under conditions of complete charge collection are displayed in Fig. 9. Unfortunately it is not possible to follow the electron-mobility values obtained in this regime above 350 K since the transit time becomes too short ($< 5 \times 10^{-7}$ s) to follow accurately. Of course, the transit time can be lengthened by using lower applied fields; however, for sample 217, this then gives incomplete charge collection ($E > 1 \times 10^4$ V/cm) and inaccuracies in the derived mobility value (Fig. 8). In order to test the predictions of the Tiedje and Rose⁴ model in the temperature range $T \geq T_c$, a sample showing complete charge collection at fields $\sim 10^2$ V/cm is needed.

C. Trapping parameters for sputtered *a*-Si:H

In this section we use the data presented in Sec. III A to obtain values of carrier lifetimes with respect to trapping at defect states. Combining these with the values of defect densities obtained from space-charge-limited-current

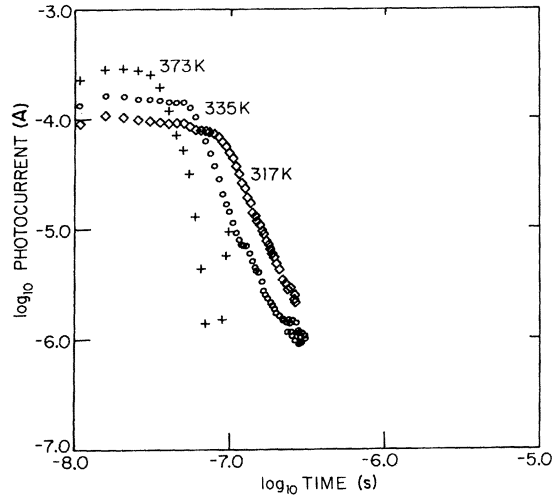


FIG. 9. High-temperature phototransients in sample 217B in the regime of complete charge collection ($V_{app} = 24$ V).

(SCLC) measurements we are able to obtain estimates of the capture cross section of the dominant defect in sputtered *a*-Si:H. The charge-collection experiments described earlier have recently been used to extract carrier lifetimes in glow-discharge-deposited *a*-Si:H,⁸ and it is of interest to see if sputtered material is described by the same parameters.

In the TOF experiment, the charge induced on the collecting electrode by the drift of n electrons a small distance dx is

$$dq = ne(dx/d),$$

where d is the electrode spacing. Now if carrier loss occurs during the transit of charge, the number of electrons still free a time t after excitation is

$$n = n_0 e^{-t/\tau_D},$$

where τ_D is the deep trapping time. With the use of $dx = \mu_D E dt$, where μ_D is the drift mobility, here taken to be approximately independent of time, the total charge displacement is found by integrating dq from zero to t ,

$$q(t) = \frac{n_0 e \mu_D E}{d} \int_0^t e^{-t'/\tau_D} dt',$$

so that the total collected charge Q in the time of the experiment is given by

$$Q = \frac{n_0 e \mu_D \tau_D E}{d} (1 - e^{-d/\mu_D \tau_D E}),$$

where $n_0 E$ can be set equal to the amount of injected charge Q_0 . In the limit of range limitation ($\mu_D \tau_D E < d$) we then have

$$Q = Q_0 (\mu_D \tau_D E / d). \quad (8)$$

This relationship can be used to derive the $\mu_D \tau_D$ product of our films using the results of the charge-collection experiments in Fig. 2. The parameters that we derive are displayed in Table I. A rough estimate of τ_D can also be made by using the transit time corresponding to a voltage at which algebraic current decays are observed. Of course the exact analysis is not expected to be totally applicable due to the dispersive nature of the transport and the distribution of defect states expected in this material. If τ_D is controlled by the density of defect states then we might expect that $\mu_D \tau_D \propto [N(E_F)]^{-1}$, since the shallow-trap-dependent μ_D should not, and experimentally does not, depend on the deep-defect-state density. Table I reveals that this relationship is qualitatively followed if we use the values of $N(E_F)$ that we obtain from SCLC fittings. SCLC would seem to provide a very simple means of characterizing device-grade *a*-Si:H in the Schottky-diode configuration. The analysis of both $[C(V) | C(\omega)]$ and SCLC measurements used to obtain the values in Table I is discussed in detail by Weisfield.¹⁵

From the experimental electron-lifetime values that we have found it is possible to use the formula

$$\sigma v = \mu_0 / \mu_D \tau_D N_{EF} \quad (9)$$

to estimate the capture cross section σ of the dominant defect responsible for carrier loss. In this formula v is the thermal velocity and μ_0 is the extended state mobility. The values to be chosen for μ_0 and v are model dependent. If we use $\mu_0 = 10$ and $v = 10^7$ cm/s then we obtain $\sigma = 5 \times 10^{-15}$ cm² for our sputtered *a*-Si:H films, a value which is the same as that derived for glow-discharge material.⁸ It is interesting that the same number is obtained despite the use of the dangling-bond resonance in ESR as a measure of the defect density in Ref 4, whereas our value is obtained from SCLC estimates. Since the capture cross section of a defect state is dependent on the charge

TABLE I. Property measurements and derived trapping parameters for the samples used in this study.

Sample no.	$N(E_F)$ [$C(v) C(\omega)$] (cm ⁻³ eV ⁻¹)	$N(E_F)$ SCLC (cm ⁻³ eV ⁻¹)	$\mu_D \tau_D$ Q vs E (cm ² V ⁻¹)	μ_D (250 K) I vs t (cm ² V ⁻¹ s ⁻¹)	τ_D (250 K) I vs t (s)	$\mu_D \tau_D N_{EF}^a$ (cm ⁻¹ V ⁻¹)
217	1.5×10^{16}	2.4×10^{15}	3.6×10^{-8}	7.0×10^{-2}		$8.6 \times 10^{+7}$
214	1.25×10^{16}	1.0×10^{16}	1.8×10^{-8}			$1.8 \times 10^{+8}$
195	1.0×10^{16}	9.0×10^{15}	2.0×10^{-8}	6.0×10^{-2}	2.8×10^{-7}	$1.8 \times 10^{+8}$
213	4.0×10^{16}	2.5×10^{16}	7.3×10^{-9}		$< 10^{-7}$	$1.8 \times 10^{+8}$

^a N_{EF} values obtained from SCLC measurements.

state (positive, neutral, or negative) and the microscopic nature of the defect center, it is likely that the dominant defect in *a*-Si:H is independent of preparation and an electron added to the center will be localized to the same extent.

Carrier transport at room temperature and below is interrupted by trapping from and release to conducting states. The resulting immobilization time at a localized state below the conduction band will then increase with decreasing temperature since the thermal emission time increases. This means that the total electron lifetime with respect to deep trapping will increase in the same manner as the drift mobility decreases as the temperature is lowered. It is also apparent from Eq. (2) that by measuring any temperature dependence of the collected charge (proportional to $\mu_D \tau_D$) for a given applied field we can test the temperature dependence of σv , and so of σ . The results of such a test on samples 213 and 217 for fields yielding both complete and incomplete charge collection are displayed in Table II. There is no evident temperature dependence of $\mu_D \tau_D$ and so we conclude that σ is independent of temperature. It is possible to write the cross section in the form¹⁶

$$\sigma = \sigma_\infty e^{-E_\infty/RT},$$

where $-E_\infty$ is the activation energy associated with capture. In our case E_∞ is zero. This is consistent with the capture of an electron at a neutral center either by tunneling from shallow states or directly from extended states.

D. Phototransients in P-doped sputtered *a*-Si:H

It is now well known that incorporation of phosphorus into *a*-Si:H, while shifting the Fermi level toward the conduction band introduces both shallow donor levels and states deep in the pseudogap.¹⁷ Furthermore the P doping decreases the free-hole lifetime, while leading to an increased electron lifetime, which is probably the result of

hole trapping. The increased electron lifetime should be apparent in TOF experiments. Here we present preliminary results which show that this is indeed the case; more detailed results will appear in a future publication. In principle, charge-collection experiments for both electrons and holes, carried out on samples whose Fermi levels have been shifted and gap density of states changed by P incorporation, should provide detailed information on the energy distribution of the states responsible for electron and hole capture.

In Fig. 10 we show a TOF photocurrent transient in a moderately phosphorus-doped *a*-Si:H film. [$C(V) | C(\omega)$] measurements on similar samples suggest that $N_{EF} \sim 5 \times 10^{17} \text{ cm}^{-3} \text{ eV}^{-1}$ for the film under study here. Sample 213 [Fig. 1(c)] which also had such a high defect-state density revealed a photocurrent that decayed rapidly giving an approximate t^{-1} decay at 250 K. In fact, a t^{-1} decay is expected for a MT and release transport process in a distribution of states that is constant in energy. So we might expect the TOF photocurrents in phosphorus-doped material to be dominated by carrier loss to deep states. However, Fig. 10 shows that this is not the case. The fact that a transit time is observed at all means that the free-electron lifetime has increased when compared to undoped samples which also have high state densities. The cause is the filling of the defect states responsible for the deep trapping (the dangling bonds) through the raising of the Fermi level.

The electron drift mobility at 220 K obtained from Fig. 10 is $1.7 \times 10^{-3} \text{ cm}^2 \text{ V}^{-1} \text{ s}^{-1}$. This compares with an electron-mobility value of $4.0 \times 10^{-2} \text{ cm}^2 \text{ V}^{-1} \text{ s}^{-1}$ for the undoped sample, 217 (Fig. 8), at the same temperature. The value of α_{init} obtained from Fig. 10 is 0.5, lower than the value of 0.7 obtained at the same temperature in undoped material. Both the lower μ_D and lower α_i suggest that P incorporation has changed the tail-state distribution.

TABLE II. Collected charge derived from $\int I dt$ vs temperature showing the invariance of the product σv to temperature. Results for sample 217 are recorded under conditions of complete charge collection, those on sample 213 for incomplete charge collection.

Sample	Temperature (K)	Charge collection $\int I dt$ (C)
217	250	3.0×10^{-11}
	240	2.9×10^{-11}
	220	2.9×10^{-11}
	170	3.4×10^{-11}
	150	2.15×10^{-11}
	140	2.35×10^{-11}
	110	8.1×10^{-12}
213	235	1.6×10^{-11}
	220	2.7×10^{-11}
	200	1.9×10^{-11}

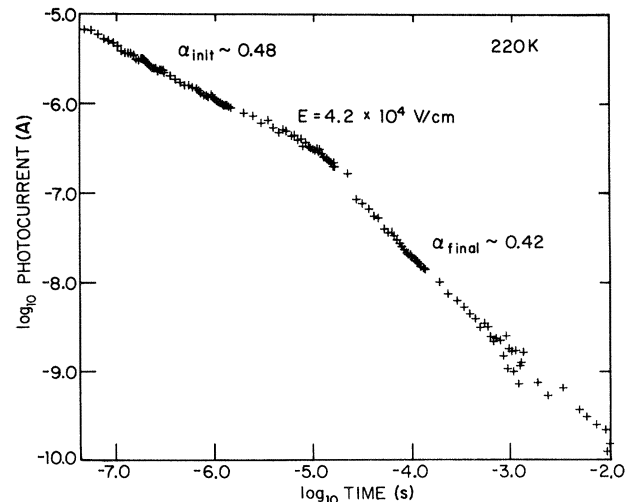


FIG. 10. Photocurrent transient for electrons in an *a*-Si:H sample doped with phosphorus. Measurement temperature was 220 K. Sample thickness was $\sim 2.5 \mu\text{m}$.

E. Comparison of photocurrent decays observed in TOF with those obtained in coplanar geometry

We know that at any time following pulsed excitation, electron mobilities are higher than hole mobilities. This means that electrons will be providing the main contribution to $I(t)$ if both carriers are drifting. In Sec. III C we reported that the deep trapping electron lifetimes seen in TOF experiments above 250 K are smaller than 10^{-6} s, and we expect similar carrier losses and photocurrent decreases in the coplanar photocurrent experiments. The results at several temperatures are shown in Fig. 11 for a glow-discharge-prepared sample co-deposited with the TOF sample of Fig. 4. At 310 K we find a fast decay of the photocurrent which is independent of the intensity of the exciting light. This is consistent with the results of Fig. 4 and is exactly what is expected for carrier loss to deep states. It was also apparent from Sec. III C that the electron lifetime increases with decreasing temperature as a result of the lengthened emission time from shallow localized states. We associate this with the increasingly persistent photocurrent observed in Fig. 11 as the temperature is lowered. As in the TOF experiment there will be a wide distribution of trapping times, so we do not expect $I(t)$ to be of the form $e^{-t/\tau}$. We can obtain an approximate measure of the average electron lifetime τ_{av} as the time at which the current decay is t^{-1} . When we do this as a function of temperature we find that the determined τ_{av} increases with decreasing temperature in the same way as the electron drift mobility measured by TOF, exactly as expected.

At low temperatures before deep trapping or recombination takes place the time dependence of the photocurrent should be the same as that measured in TOF experiments. This is the situation in $a\text{-As}_2\text{Se}_3$.¹⁰ So at low temperature an algebraic current decay should be observed whose slope should increase with decreasing temperature.

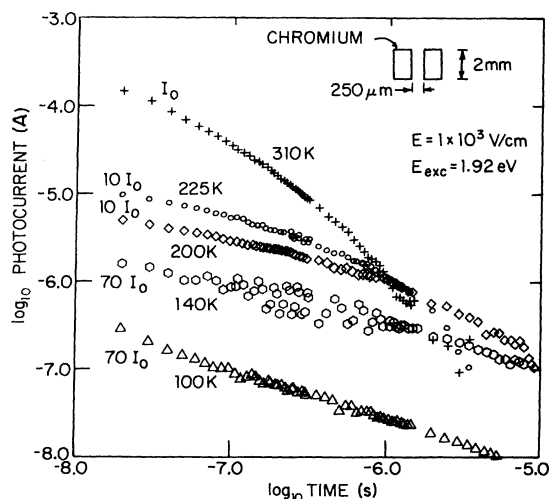


FIG. 11. Coplanar photocurrent decays in undoped glow-discharge $a\text{-Si:H}$. Relative light intensities used at each temperature are shown. I_0 is estimated to correspond to approximately $1 \mu\text{J}/\text{cm}^2$.

The results in Fig. 11 are in qualitative agreement with this though exact algebraic decays are not seen. Further studies are necessary to determine the importance of the surface trapping on the dispersive transport process. The mobility of electrons is so high that diffusion to the surface is a strong possibility at high temperatures.

Surface band-bending effects are expected to be more important in undoped $a\text{-Si:H}$ films than in phosphorus-doped material since the Fermi level can be pinned by the high density of states in the latter. We have made coplanar $I(t)$ measurements on a moderately phosphorus-doped sample that was co-deposited with the TOF sample of Fig. 10. The results at a single excitation intensity are shown in Fig. 12. At temperatures above 180 K the decays are intensity dependent indicating that bimolecular recombination is occurring. However, below 180 K bimolecular recombination time is so long that its influence on the photocurrent decay is negligible. In this regime the current decays are found to be algebraic and indeed at 140 K the same decay is measured in TOF as in the present experiment.

In summary, it is clear that the results of both TOF and coplanar photocurrent studies show changes in P-doped samples. The derived dispersion parameters are changed and the electron mobility is much reduced. Apparently P-doping alters the distribution of shallow trapping states probed in these experiments, a result that is expected from simple considerations of the energy levels of P donors and the state distribution in the tail attributed to disorder.

IV. CONCLUSIONS

Through a combination of observation of photocurrent transients and charge collection versus applied field in the

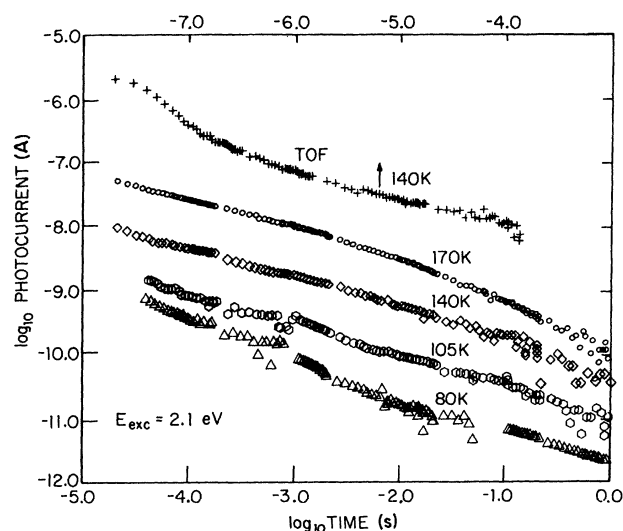


FIG. 12. Coplanar photocurrent decays in phosphorus-doped sputtered $a\text{-Si:H}$ recorded at a single intensity. Also shown is the electron phototransient recorded in the TOF configuration on a co-deposited sample run. Incident intensity for the photocurrent decays is estimated to be $\sim 12 \mu\text{J}/\text{cm}^2$. Curves are arbitrarily displaced relative to each other.

TOF experiments we have shown that for the correct determination of the dispersion parameters relevant to the understanding of transport in *a*-Si:H, all excess injected carriers must successfully transit the sample. We have identified both transport through the high-field-barrier region and carrier loss to deep traps as influencing the current decays observed due to drifting carriers in the TOF experiment. Our use of an insulating layer between the *a*-Si:H film and the top metal contact gives space-charge-free samples permitting the identification of surface trapping at low fields. The currents measured in such structures cannot be due to the relaxation of any space charge and so are consistent with carrier drifts.

Under conditions of complete charge collection we have made measurements of α_{init} and α_{final} for electrons in sputtered *a*-Si:H. We find a linear variation of α_{init} with temperature consistent with transport model involving multiple trapping and release in an exponential distribution of conduction-band-tail states. The steepness of this distribution for sputtered *a*-Si:H films is only slightly different from that obtained in glow-discharged-prepared films. Below 130 K our measurements indicate that electrons in the conduction-band-tail states move by a new transport process.

Our charge-collection experiments give values for the

$\mu_D \tau_D$ product in sputtered *a*-Si:H that vary inversely with the density of deep states. We derive a value of $5 \times 10^{-15} \text{ cm}^{-2}$ for the capture cross section of the dominant defect and show this is independent of temperature. Doping *a*-Si:H with phosphorus increases the lifetime of electrons due to the movement of the Fermi level through the dangling-bond defect states. Our preliminary measurements on moderately phosphorus-doped *a*-Si:H suggest that the conduction-band-tail state distribution is modified with the addition of donor atoms.

We show measurements of photocurrents in the coplanar geometry using uniform optical excitation between the electrodes. The photocurrents observed in this case on undoped *a*-Si:H are consistent with dominating electron carrier loss at 300 K. Below 300 K the electron lifetime increases leading to persistent photocurrents.

ACKNOWLEDGMENTS

We thank H. Lüne, Dr. S. Oguz, Dr. B. von Roedern, and Dr. R. L. Weisfield, all of whom helped the progress of this work. Financial support was provided by the U. S. Department of Energy under Contract No. DE-AC-0282ER12064.

¹W. E. Spear, *J. Non-Cryst. Solids* **1**, 197 (1969).

²See, for references, G. Pfister and H. Scher, *Adv. Phys.* **27**, 747 (1978).

³H. Scher and E. W. Montroll, *Phys. Rev. B* **1**, 4491 (1973).

⁴T. Tiedje and A. Rose, *Solid State Commun.* **37**, 49 (1980).

⁵P. B. Kirby and W. Paul, *Phys. Rev. B* **25**, 5373 (1982).

⁶T. Tiedje, T. D. Moustakas and J. M. Cebulka, *J. Phys. (Paris) Colloq.* **42**, C 4-155 (1981).

⁷K. Hecht, *Z. Phys.* **77**, 235 (1932).

⁸R. A. Street, *App. Phys. Lett.* **41**, 1060 (1982).

⁹J. Orenstein, M. A. Kastner, and V. Vaninov, *Philos. Mag. B* **46**, 23 (1982).

¹⁰B. A. Khan, M. A. Kastner, and D. Adler, *Solid State Commun.* **45**, 187 (1983).

¹¹W. Paul and D. Anderson, *Solar Energy Mater.* **5**, 229 (1981).

¹²Theories of dispersive transport predict that $t_T \propto E^{-1/\alpha}$ (see Ref. 2 for details).

¹³T. Datta and M. Silver, *Solid State Commun.* **38**, 1067 (1981).

¹⁴T. Tiedje, J. M. Cebulka, D. L. Morel, and B. Abeles, *Phys. Rev. Lett.* **46**, 1425 (1981).

¹⁵R. L. Weisfield (unpublished).

¹⁶C. H. Henry and D. V. Lang, *Phys. Rev. B* **15**, 989 (1977).

¹⁷D. A. Anderson, G. Moddel, and W. Paul, *J. Non-Cryst. Solids* **35-36**, 6, 345 (1980).